J Nanostruct 16(2): 1790-1799, Spring 2026

RESEARCH PAPER

Structural, Optical, and Antibacterial Properties of PEO/PANI Nanocomposites Doped with WO_3, Cr_2O_3, and NiO Nanoparticles

Rusul K. Mohammed Jasim *, Mohammed Hadi Shinen, Saba Abdulzahra Obaid

Department of Physics, College of Science, University of Babylon, Iraq

ARTICLE INFO

Article History:
Received 29 December 2025
Accepted 27 March 2026
Published 01 April 2026

Keywords:
Antibacterial Properties
FESEM
Nano oxides
Polymer

ABSTRACT

Four different nanocomposite solutions were prepared by solution casting binary polymer blends composed of polyethylene oxide (PEO) and polyaniline (PANI), incorporating metal oxide nanoparticles (WO_3, Cr_2O_3, and NiO) at controlled concentrations. The objective was to evaluate the influence of oxide incorporation on the structural, optical, and antibacterial characteristics of the resulting films. X-ray diffraction (XRD) patterns confirmed the semi-crystalline nature of the blends and revealed slight modifications in crystallinity upon oxide addition, indicating good nanoparticle dispersion within the polymer matrix. Fourier transform infrared (FTIR) spectroscopy demonstrated strong intermolecular interactions and possible hydrogen bonding between the functional groups of the polymers and the metal oxides. UV–Visible spectroscopy showed enhanced optical absorption and reduced band gap values after doping, reflecting improved electronic transitions. Antibacterial activity tests exhibited clear inhibition zones against S. aureus (6–18 mm) and E. coli (6–21 mm), confirming promising potential for optoelectronic and biomedical applications. all materials prepared to give a good promising result.

How to cite this article
Jasim R., Shinen M., Obaid S. Structural, Optical, and Antibacterial Properties of PEO/PANI Nanocomposites Doped with WO_3, Cr_2O_3, and NiO Nanoparticles. J Nanostruct, 2026; 16(2):1790-1799. DOI: 10.22052/JNS.2026.02.030

INTRODUCTION

The need to develop new and effective materials with antibacterial properties has become urgent, given the continuous increase in bacterial resistance to traditional antibiotics. Therefore, polymers have received significant attention in research circles due to the possibility of modifying their properties. They can be employed as matrices support and maintain active nanoparticles, as active chemicals, or as carriers of antibacterial agents. For instance, two of the most popular polymers in this sector are polyaniline (PANI) and polyethylene oxide (PEO) [1].Since adding nanoscale oxides to polymers increases their capacity to produce reactive oxygen species (ROS), cause proteins and DNA within cells to oxidize, they can be utilized as active chemicals [2].Oxides such as tungsten oxide (WO_3), chromium oxide (Cr_2O_3), and nickel oxide (NiO), are commonly used to change the thermal stability, electrical conductivity, and antibacterial activity of polymers [3]. Due to its large energy

* *Corresponding Author Email: rusulkadhom7@gmail.com*

gap, tungsten oxide can absorb light and react with it to generate reactive oxygen species [4]. Free radicals are produced as a result of this electrical excitation, which breaks down the bacterial cell wall [5]. Chromium trioxide's antibacterial action, however, is ascribed to its capacity to modify the polymer's surface characteristics, which lessens bacterial adhesion to the material's surface [6]. Additionally, it interferes with the bacterial cell membrane's permeability, which stops the bacteria from preserving their ionic equilibrium. [7]. These species attach to the bacterial cell wall due to their positive surface charge, which also facilitates their ability to break down proteins and cellular membranes. Furthermore, doping the polymers with it helps to boost the polymer material's efficiency [8]. Two common forms of pathogenic bacteria have been identified, and bacteria are among the most prevalent and significant microbes impacting human health.

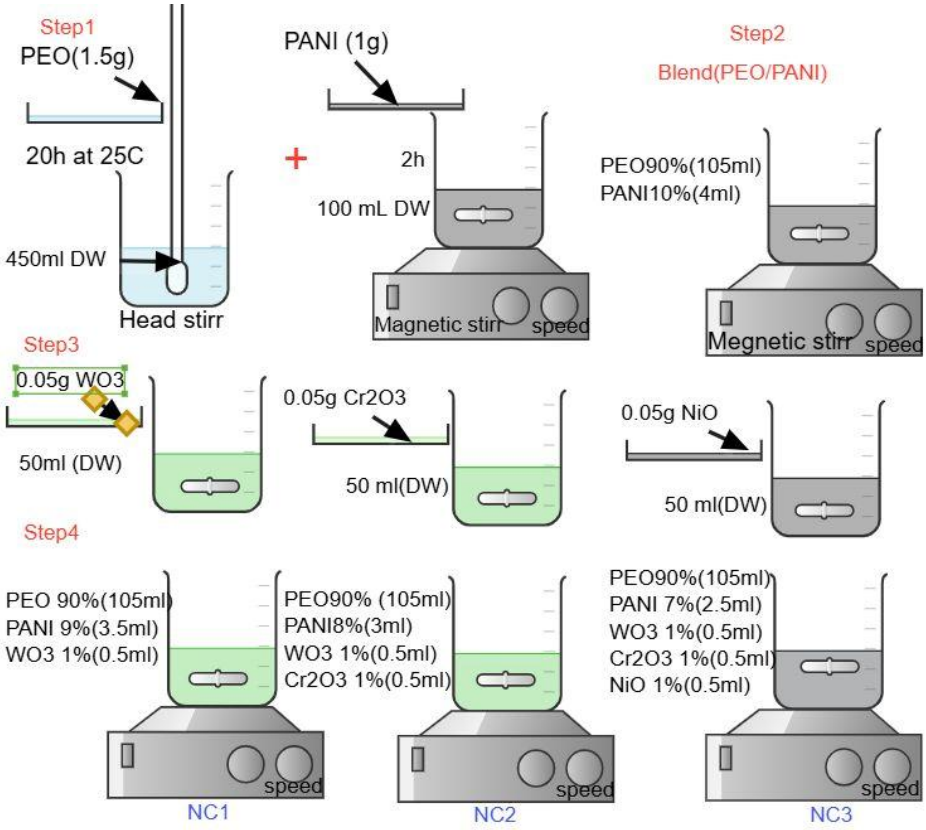

Fig. 1. Schematic of the experimental process in this study.

Table 1. Material Properties for PEO/PANI blend Synthesis with WO_3, Cr_2O_3, and NiO.

Sample	Mass(g)	distilled water (mL)	molecular weight (g/mol)	Company
PEO	1.5	450	3,000,000	Panichem Co., Ltd., South Korea
PANI	1	100	150,000	Cheng Du Micxy Chemical Co., Ltd., China
WO_3	0.05	50	231.84	Hongwu International Group Ltd. China
Cr_2O_3	0.05	50	151.99	Telligent Materials Pvt. Ltd., India
NiO	0.05	50	74.69	Sky Spring Nanomaterials, Inc. The United States

Escherichia coli (E· coli) is a gram-negative bacterium [9]. The most common E. coli infection is a urinary tract infection, but individuals can also contract intestinal infections by consuming contaminated food (such as undercooked ground beef), coming into contact with infected animals, or drinking contaminated water.[10]. However, Staphylococcus aureus S.aureus) is a gram-positive bacterium that can cause post-operative wound infections and mild skin diseases [11]. Polymers are employed in the production of antimicrobial dressings that aid in wound healing and infection prevention, as well as in the coating of medical devices, such as catheters [12], needles [13], and other [14]. They are also used in food packaging to prevent bacterial growth on food, as well as in drug delivery systems [15], for treating fabrics [16], and in the production of medical clothing [17], masks [18], and bedding [19]. In addition, they are used in air and water filters found in laboratories and hospitals [20]. Antibacterial polymers are therefore crucial in the fight against bacteria's growing resistance to conventional antibiotics [21].

MATERIALS AND METHODS

Materials

Polyethylene oxide (PEO, Mw ≈ 3,000,000), polyaniline (PANI, emeraldine salt), tungsten trioxide (WO_3), chromium (III) oxide (Cr_2O_3), and nickel (II) oxide (NiO) nanopowders were purchased from commercial suppliers with purity ≥99%. Every chemical was used exactly as it was delivered, requiring no additional purification. The

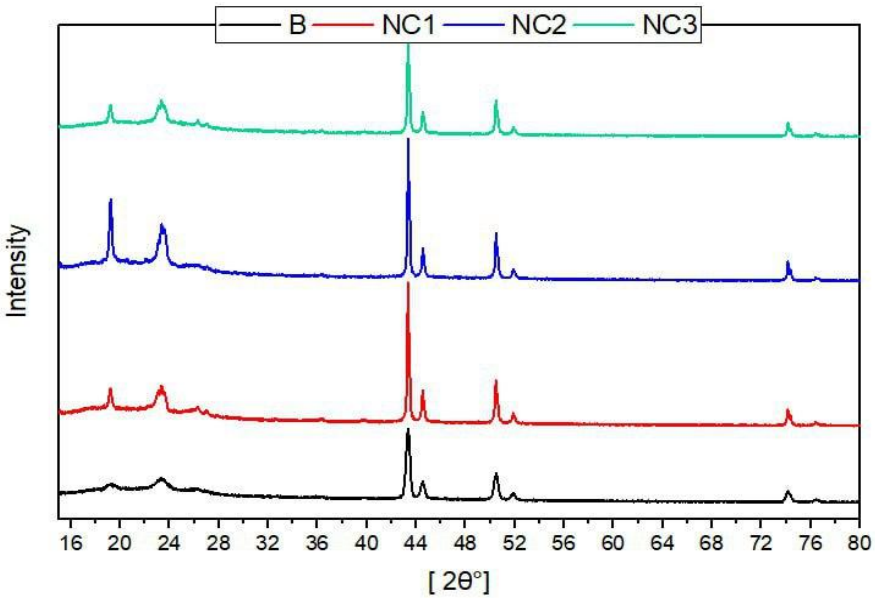

Fig. 2. X-ray diffraction (XRD) was recorded at 2θ° for the polymer blend B and its corresponding nanocomposites NC1, NC2, and NC3.

Table 2. Concentration of PEO/PANI blend and Nanocomposites.

Polymer	PANI	WO_3	Cr_2O_3	NiO
PEO 90%	10%	-	-	-
PEO 90%	9%	1%	-	-
PEO 90%	8%	1%	1%	-
PEO 90%	7%	1%	1%	1%

solvent utilised was distilled water (DW).

Preparation of a blend of PEO/PANI Solution

The polymer blend was prepared by dissolving 1.5gm of PEO in 450 mL of DW under magnetic stirring at ~20 °C until complete dissolution (~20h). Separately, 1.0 g of PANI (emeraldine base) was ultrasonically dispersed in 100 mL of DW for 2 h. The two solutions were then combined and stirred for an additional 2 h to form a homogeneous PEO/

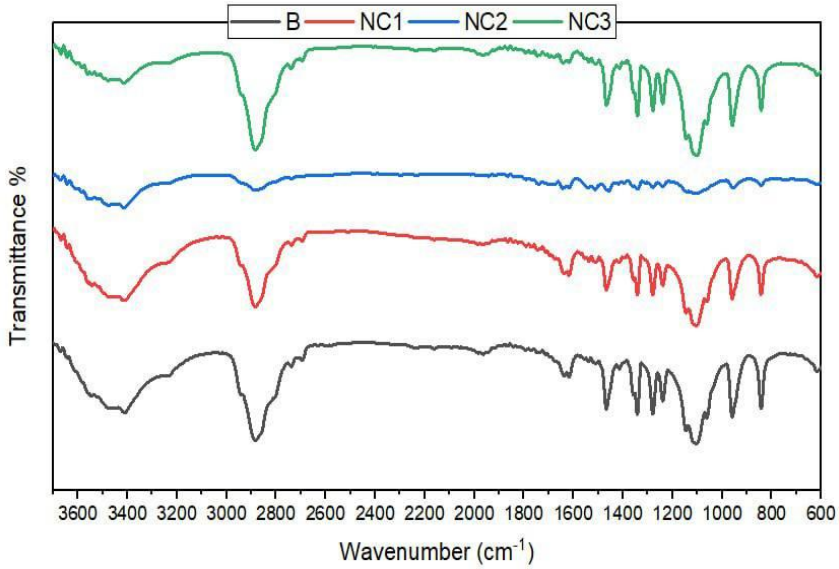

Fig. 3. FTIR spectrum for ternary blend (PEO/PANI) and nanocomposites

Table 3. provides an overview of the average lattice strain (ε), diffraction angle (2θ), FWHM (β), d-spacing (d), and average crystallite size(D), for both blended polymers and NC1, NC2, and NC3.

2θ (°)	d(nm)	β (°)	D (nm)	ε ×10⁻³
19.2144	4.6155	0.2683	30.029	6.9165
23.3504	3.8065	0.9093	8.992	19.1995
26.2984	3.3761	0.3155	25.86	5.8922
43.3374	2.0222	0.2009	42.54	2.2068
44.5254	1.808	0.2165	39.645	2.3079
50.5654	1.7500	0.2541	34.566	2.3524
51.8624	1.7615	0.2525	34.566	2.2662
76.3924	1.2457	0.1963	51.492	1.0887
89.9444	1.0899	0.2124	52.878	0.9275
92.9474	1.0624	0.1692	68.175	0.7013
95.1584	1.0434	0.1869	63.006	0.7452

PANI blend.

Preparation of Nanocomposites

Metal oxide nanopowders (WO_3, Cr_2O_3, and NiO) were dispersed individually in 50 mL of distilled water by ultrasonication (40 kHz, 60 min). Each dispersion containing 0.05 g of oxide was gradually added to the PEO/PANI blend under continuous stirring for 3 h, followed by ultrasonication for 15 min to ensure uniform nanoparticle dispersion mixtures. These were cast into clean Petri dishes and dried slowly at ~20 °C for 10 days to obtain uniform thin films, as shown in Fig. 1 and Table 1 summarizes the mass of each component used to prepare PEO/PANI nanocomposite samples doped with WO_3, Cr_2O_3, and NiO oxides while the compositions are shown in Table 2.

RESULTS AND DISCUSSION

X-Ray Diffraction

The pure blend polymer (B) exhibits broad and weak diffraction peaks, indicating its predominantly amorphous or semi-crystalline nature. This is typical for polymeric systems such as PEO and PANI, where the degree of crystallinity is limited by chain entanglement and structural disorder. Upon incorporation of metal oxide nanoparticles, the XRD patterns of the nanocomposites (NC1, NC2, and NC3) exhibit a series of sharp and intense diffraction peaks, confirming the presence of crystalline phases corresponding to the added oxides. The emergence of these peaks is indication of the successful embedding of the oxide [22]. The increased intensity and sharpness of the diffraction peaks with the progression from NC1 to NC3 suggest enhanced crystallinity, which can be attributed to the nucleating effect of the nanoparticles, which promotes local ordering of polymer chains. incorporated oxides' intrinsic crystalline nature dominates the XRD response. The incorporation of nanostructured oxides not only improves the crystallinity of the system but also is expected to enhance its functional properties, including electrical conductivity,

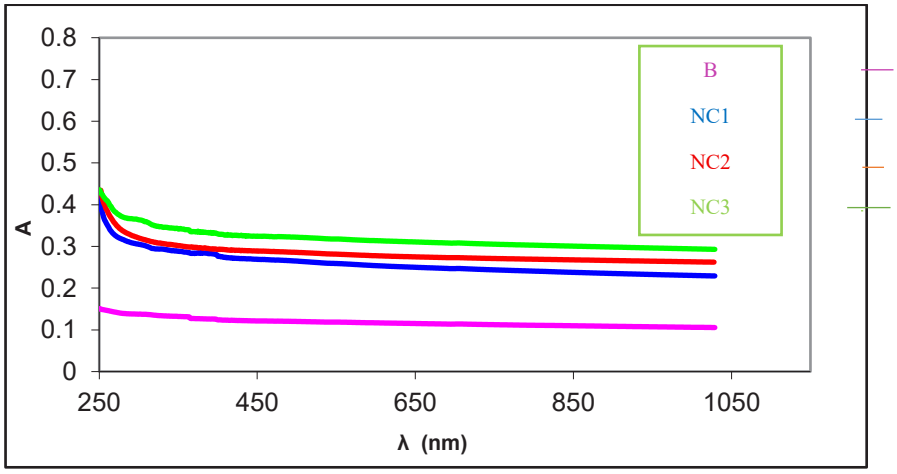

Fig. 4. The Absorption for PEO/PANI Blend and Nanocomposites

Table 4. FTIR functional groups and related peaks.

Peak, cm^{-1}	Functional groups	details	Ref.
3200-3600	O–H stretching (PEO) and N-JH stretch (PANI)	strong	[23]
2883-2885	C-H or CH2 and indicated hydrogen bonding	medium	[26]
1103-1062	Stretching C–O–C vibration	strong	[27]
1000-1111	CH bending PEO/ stretching C-O/ C=C (benzene ring)	strong	[28]
842-420	M–O stretching	medium	[29]

thermal stability, and gas sensing performance, as shown in Fig. 2 [23]. In Table 3, calculations showed that the crystalline size of samples loaded with nanocomposites NC1, NC2, and NC3and blend.

FTIR Fourier transform infrared spectroscopy

In Fig. 3, FTIR spectra of the synthetic polymers with or without the respective NCs after doping nanomaterials in the ternary blended polymers have been shown. Infrared spectrum analysis of polymer (B) (ternary blended) showed noticeable peaks of functional groups 3414,2883,1103,1467,960,842,617 and 470 cm−1. The formation of robust hydrogen bonds due to the existence of numerous hydroxyl and carboxyl groups was indicated by the stretching vibration of –OH bands derived from PEO [22]. Table 4 shows FTIR spectra results.

Optical properties

Absorption (A)

Absorbance values rise as a function of wavelengths, as seen in Fig. 4. In the infrared range (200-1100 nm) and near to it, the absorbance rises with increasing doping of nanocomposites for all of the produced films. According to the results in Fig. 4. Thin film absorbance declines with increasing wavelengths, which is why PEO/PANI were found to have the lowest absorbance spectrum. The best results were obtained by adding nanocomposite films. PEO/PANI blend shows a primary absorption peak that redshifts, or shifts toward higher wavelengths, in the doped samples. This change implies that oxide incorporation is responsible for the creation of localized electronic states within the bandgap. All the samples show a significant increase in absorption intensity, indicating an intense light–matter interaction and improved

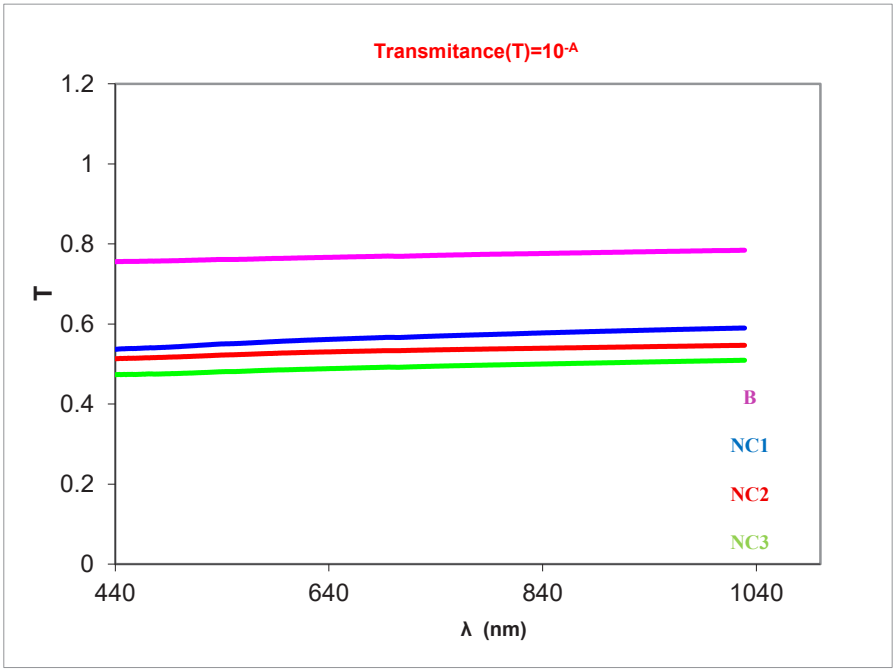

Fig. 5. Transition for Blend and Nanocomposites.

Table5. Values of energy gap, PEO/PANI Blend, and Nanocomposites.

Material	E_g (eV)
B	2
NC1	2.5
NC2	1.9
NC3	1.6

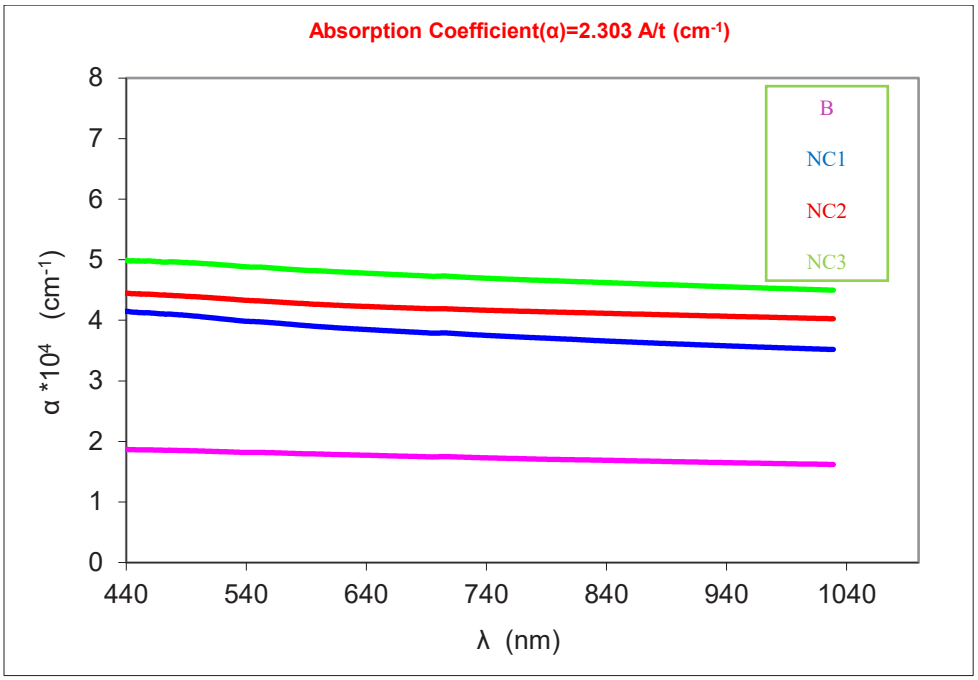

Fig. 6. Absorption coefficient of blend polymer and Nanocomposites.

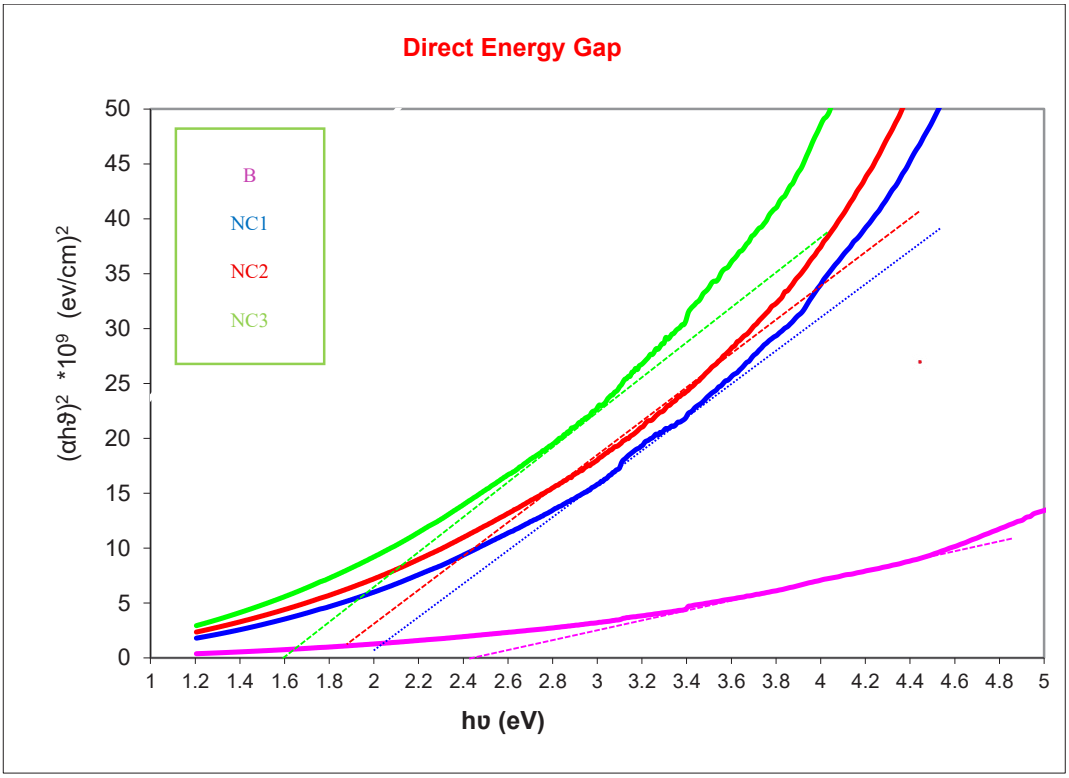

Fig. 7. Energy gap of PEO/PANI Blend and Nanocomposites.

optical activity.

Transition (T)

At a wavelength of roughly 200–1100 nm, the blend's transmittance spectra and those of its nanocomposites doped with WO_3, Cr_2O_3 and NiO, were measured. According to the results, the addition of metal oxide nanoparticles appears to reduce transmittance, suggesting improved light-matter interaction in the composite materials. The highest transmittance, indicating lower optical absorption, was shown by the pure PEO/PANI blend but adding nanocomposites showed the lowest transmittance throughout the spectrum, suggesting increased absorption and/or scattering effects. Oxide doping, which creates localized

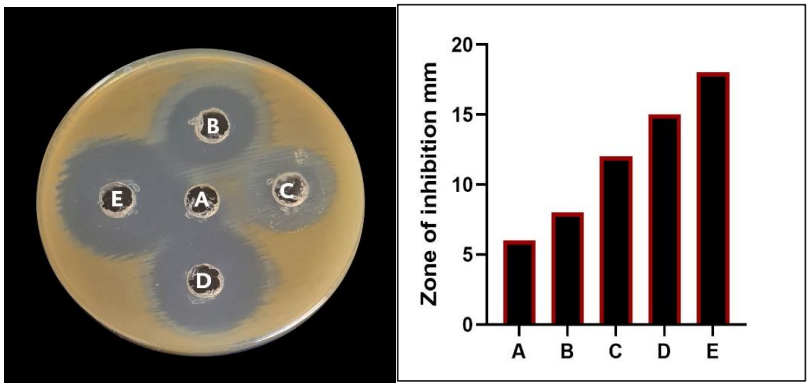

Fig. 8. The test material's antibacterial effectiveness against E. coli, A) Control., B) 12.5%, C)25 %, D) 50 %, E) 100 %.

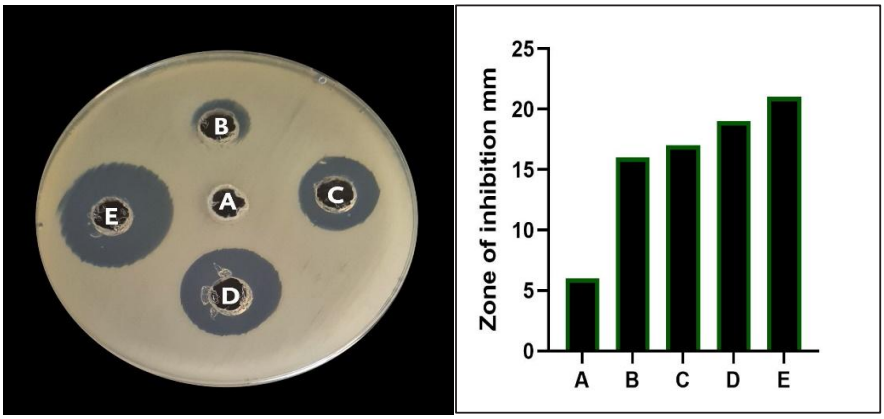

Fig. 9. The test material's antibacterial effectiveness against S. aureus A) Control., B) 12.5%, C)25 %, D) 50 %, E) 100 %.

Table 6. Analysis of Antibacterial.

Sample	Concentration%	S. aureus	E. coli
Control	-	6	6
Blend	12.5	8	8
NC1	25	12	16
NC2	50	15	17
NC3	100	21	18

energy levels inside the bandgap to encourage photon absorption, explains this effect. Since the observed decrease in transmittance suggests enhanced optical activity and possibly a reduced optical bandgap, the doped composite is a viable option for use in optoelectronic devices, and antibacterial surfaces exposed to light.

The Coefficient of Absorption (A)

The optical absorption coefficient is shown Fig. 6 All thin films with values $\alpha>10^4\,cm^{-1}$ in the visible range have a direct optical energy gap [30]. The optical absorption coefficient (α) was calculated using the relation α=2·303 A/t Where A is the absorbance and t is the film thickness [31]. The film thickness measured using a digital micrometer was approximately 100 ± 10 µm.

Energy gap (Eg)

The optical bandgap *Eg* was determined using Tauc plots Fig. 7. Doping reduced Eg due to the formation of localized energy levels, facilitating low-energy electronic transitions. The Eg values are presented in Table 5, confirming improved photo-responsiveness in doped samples.

Antibacterial activity

The bacteria were cultured in a Mueller-Hinton (MH) agar (20 mL) with an inoculation loop [32] was used at a temperature of 37°C [33]. A small amount is placed in a Petri dish and holes are made with a diameter of six mm [34]. Several concentrations were taken, and the diameter of the inhibition zone was calculated for each concentration. The antibacterial efficiency of the PEO/PANI and its nanocomposites was evaluated against Escherichia coli (gram-negative) and Staphylococcus aureus (gram-positive) [35]. Using the agar diffusion method (Figs. 8 and 9). The inhibition zones are summarized in Table 6. The PEO/PANI blend exhibited moderate antibacterial activity. Upon doping with metal oxides, a significant improvement was observed. The enhanced antibacterial performance can be attributed to several factors: Transition nano oxides that generate reactive oxygen species (ROS) [36], electrostatic interaction between positively charged polyaniline (PANI) and negatively charged bacterial membranes, resulting in the disruption of cell wall [37] and the surface area and porosity of doped samples led to the better interaction of bacteria with the nanoparticles [38].

CONCLUSION

The ternary blend polymers (PEO/PANI) and their nanocomposites (WO_3, Cr_2O_3, NiO) were successfully prepared by casting. FESEM showed rough, irregular, and agglomerated surfaces with granular structures. FTIR confirmed strong crosslinking in both polymers and nanocomposites. UV spectra showed enhanced absorbance with strong peaks from 320 to 400 nm. Antibacterial tests revealed notable inhibition against S. aureus and E. coli. These results indicate that oxide-doped PEO/PANI blends have promising structural, optical, and biological properties for optoelectronic and antimicrobial applications.

CONFLICT OF INTEREST

The authors declare that there is no conflict of interests regarding the publication of this manuscript.

REFERENCES

1. Muxika A, Etxabide A, Uranga J, Guerrero P, de la Caba K. Chitosan as a bioactive polymer: Processing, properties and applications. Int J Biol Macromol. 2017;105:1358-1368.
2. Guo L, Yuan W, Lu Z, Li CM. Polymer/nanosilver composite coatings for antibacterial applications. Colloids Surf Physicochem Eng Aspects. 2013;439:69-83.
3. Perelshtein I, Lipovsky A, Perkas N, Gedanken A, Moschini E, Mantecca P. The influence of the crystalline nature of nano-metal oxides on their antibacterial and toxicity properties. Nano Research. 2014;8(2):695-707.
4. Thanakkasaranee S, Kasi G, Kadhiravan S, Arumugam A, Al-Ghanim KA, Riaz MN, et al. Synthesis of Tungsten Oxide Nanoflakes and Their Antibacterial and Photocatalytic Properties. Fermentation. 2023;9(1):54.
5. Warsi A-Z, Aziz F, Zulfiqar S, Haider S, Shakir I, Agboola PO. Synthesis, Characterization, Photocatalysis, and Antibacterial Study of WO_3, MXene and WO_3/MXene Nanocomposite. Nanomaterials. 2022;12(4):713.
6. Singh S, Bharti A, Meena VK. Green synthesis of multi-shaped silver nanoparticles: optical, morphological and antibacterial properties. Journal of Materials Science: Materials in Electronics. 2015;26(6):3638-3648.
7. Abbas MH, Hadi A, Rabee BH, Habeeb MA, Mohammed MK, Hashim A. Enhanced Dielectric Characteristics of Cr_2O_3 Nanoparticles Doped PVA/PEG for Electrical Applications. Revue des composites et des matériaux avancés. 2023;33(4):261-266.
8. Kannan K, Radhika D, Nikolova MP, Sadasivuni KK, Mahdizadeh H, Verma U. Structural studies of bio-mediated NiO nanoparticles for photocatalytic and antibacterial activities. Inorg Chem Commun. 2020;113:107755.
9. Green synthesis of NiO nanoparticles using Leucas Asperaand its antibacterial activity. Letters in Applied NanoBioScience. 2020;9(2):1033-1036.
10. Allocati N, Masulli M, Alexeyev M, Di Ilio C. Escherichia coli in Europe: An Overview. Int J Env Res Public Health. 2013;10(12):6235-6254.
11. Deurenberg RH, Stobberingh EE. The evolution of Staphylococcus aureus. Infect, Genet Evol. 2008;8(6):747-

763.
12. Keum H, Kim JY, Yu B, Yu SJ, Kim J, Jeon H, et al. Prevention of Bacterial Colonization on Catheters by a One-Step Coating Process Involving an Antibiofouling Polymer in Water. ACS Applied Materials and Interfaces. 2017;9(23):19736-19745.
13. Thakur VK, Singha AS, Thakur MK. Fabrication and Physico-Chemical Properties of High-Performance Pine Needles/Green Polymer Composites. Int J Polymer Mater. 2013;62(4):226-230.
14. Teo AJT, Mishra A, Park I, Kim Y-J, Park W-T, Yoon Y-J. Polymeric Biomaterials for Medical Implants and Devices. ACS Biomaterials Science and Engineering. 2016;2(4):454-472.
15. Sharma R, Singh H, Joshi M, Sharma A, Garg T, Goyal AK, et al. Recent Advances in Polymeric Electrospun Nanofibers for Drug Delivery. Critical Reviews in Therapeutic Drug Carrier Systems. 2014;31(3):187-217.
16. Mamdouh F, Othman H, Hassabo AG. Improving the performance properties of polyester fabrics through treatments with natural polymers. Journal of Textiles, Coloration and Polymer Science. 2024.
17. Morris H, Murray R. Medical textiles. Textile Progress. 2020;52(1-2):1-127.
18. Du H, Huang S, Wang J. Environmental risks of polymer materials from disposable face masks linked to the COVID-19 pandemic. Sci Total Environ. 2022;815:152980.
19. Karim N, Afroj S, Lloyd K, Oaten LC, Andreeva DV, Carr C, et al. Sustainable Personal Protective Clothing for Healthcare Applications: A Review. ACS Nano. 2020;14(10):12313-12340.
20. Balamurugan R, Sundarrajan S, Ramakrishna S. Recent Trends in Nanofibrous Membranes and Their Suitability for Air and Water Filtrations. Membranes. 2011;1(3):232-248.
21. Kamaruzzaman NF, Tan LP, Hamdan RH, Choong SS, Wong WK, Gibson AJ, et al. Antimicrobial Polymers: The Potential Replacement of Existing Antibiotics? International Journal of Molecular Sciences. 2019;20(11):2747.
22. Guthrie RD. Introduction to Spectroscopy (Pavia, Donald; Lampman, Gary M.; Kriz, George S., Jr.). J Chem Educ. 1979;56(10):A323.
23. Khasim S. Polyaniline-Graphene nanoplatelet composite films with improved conductivity for high performance X-band microwave shielding applications. Results in Physics. 2019;12:1073-1081.
24. Moussa I, Khiari R, Moussa A, Belgacem MN, Mhenni MF. Preparation and Characterization of Carboxymethyl Cellulose with a High Degree of Substitution from Agricultural Wastes. Fibers and Polymers. 2019;20(5):933-943.
25. Al-Hartomy OA, Khasim S, Roy A, Pasha A. Highly conductive polyaniline/graphene nano-platelet composite sensor towards detection of toluene and benzene gases. Appl Phys A. 2018;125(1).
26. Alawi AI, Al-Bermany E. Newly Fabricated Ternary PAAm-PVA-PVP Blend Polymer Doped by SiO2: Absorption and Dielectric Characteristics for Solar Cell Applications and Antibacterial Activity. Silicon. 2023;15(13):5773-5789.
27. Khurana S, Chandra A. Ionic liquid-based organic–inorganic hybrid electrolytes: Impact of in situ obtained and dispersed silica. J Polym Sci, Part B: Polym Phys. 2017;56(3):207-218.
28. Sridevi NA, Karuppasamy K, Balakumar S, Shajan XS. Structural and Ionic Conductivity Studies on Nanochitosan Incorporated Polymer Electrolytes for Rechargeable Magnesium Batteries. Chemical Science Transactions. 2012;1(2):311-316.
29. Jhansirani K, Dubey RS, More MA, Singh S. Deposition of silicon nitride films using chemical vapor deposition for photovoltaic applications. Results in Physics. 2016;6:1059-1063.
30. Tauc J, Grigorovici R, Vancu A. Optical Properties and Electronic Structure of Amorphous Germanium. physica status solidi (b). 1966;15(2):627-637.
31. Yin J, Yin Y. Definition of Time and Measurement of Time. International Photonics and Optoelectronics Meetings (POEM): OSA; 2013. p. NSa3A.31.
32. Andrews JM. Determination of minimum inhibitory concentrations. J Antimicrob Chemother. 2001;48(suppl_1):5-16.
33. Balouiri M, Sadiki M, Ibnsouda SK. Methods for in vitro evaluating antimicrobial activity: A review. Journal of Pharmaceutical Analysis. 2016;6(2):71-79.
34. Jihad MA, Noori FTM, Jabir MS, Albukhaty S, AlMalki FA, Alyamani AA. Polyethylene Glycol Functionalized Graphene Oxide Nanoparticles Loaded with Nigella sativa Extract: A Smart Antibacterial Therapeutic Drug Delivery System. Molecules. 2021;26(11):3067.
35. Synergistic Photocatalytic-Photothermal Contribution to Antibacterial Activity in BiOI-Graphene Oxide Nanocomposites. American Chemical Society (ACS).
36. Applerot G, Lipovsky A, Dror R, Perkas N, Nitzan Y, Lubart R, et al. Enhanced Antibacterial Activity of Nanocrystalline ZnO Due to Increased ROS-Mediated Cell Injury. Adv Funct Mater. 2009;19(6):842-852.
37. Celik MU, Ekici S. Polyacrylamide-polyaniline composites: the effect of crosslinking on thermal, swelling, porosity, crystallinity, and conductivity properties. Colloid Polym Sci. 2019;297(10):1331-1343.
38. Zhang L, Jiang Y, Ding Y, Povey M, York D. Investigation into the antibacterial behaviour of suspensions of ZnO nanoparticles (ZnO nanofluids). J Nanopart Res. 2006;9(3):479-489.